Formation of cyanopolyyne anions in the interstellar medium: The possible role of permanent dipoles

F. Carelli, F. A. Gianturco, R. Wester, and M. Satta

Citation: The Journal of Chemical Physics **141**, 054302 (2014); doi: 10.1063/1.4891300
View online: http://dx.doi.org/10.1063/1.4891300
View Table of Contents: http://scitation.aip.org/content/aip/journal/jcp/141/5?ver=pdfcov
Published by the AIP Publishing

Formation of cyanopolyyne anions in the interstellar medium: The possible role of permanent dipoles

F. Carelli,[1] F. A. Gianturco,[2,a)] R. Wester,[1] and M. Satta[3]
[1]*Institut für Ionenphysik und Angewandte Physik, Universität Innsbruck, Technikerstraße 25, A-6020 Innsbruck, Austria*
[2]*Scuola Normale Superiore, P.zza dé Cavalieri 7, Pisa I-56125, Italy*
[3]*CNR-ISMN and University of Rome "Sapienza," P.le Aldo Moro 5, Rome I-00185, Italy*

(Received 22 May 2014; accepted 15 July 2014; published online 4 August 2014)

The possibility of attaching near-threshold electrons to N-terminated carbon chains, like those observed in the outer envelopes of carbon-rich stars, is examined via accurate quantum chemistry orbital structures evaluation and quantum scattering analysis of the corresponding extra-electron wavefunctions at meV energies. It is shown that the differences in the signs and sizes of the permanent dipole moments which exist for both the neutral and anionic species of the C_nN series of molecules play a significant role in suggesting or excluding possible energy paths to permanent anion formations of cyanopolyynes, for which the cases with n from 1 to 7 are examined in more detail. © *2014 AIP Publishing LLC*. [http://dx.doi.org/10.1063/1.4891300]

I. INTRODUCTION

In the last few-years, the pure carbon clusters and their variants formed by adding a heteroatom X, with X = H, N, have been studied extensively by experiments and theory, with the view of understanding the observed formation of stable anions, C_nH^- or C_nN^-.[1–4] This is a series of largely linear compounds which have been repeatedly observed from a set of initially unidentified lines in carbon-rich stars like IRC+10216 and from further laboratory confirmations of their origin.[5–9]

From the structural viewpoint, their corresponding anions from neutral radicals, e.g., C_nN^- species, have been also extensively investigated using high-level quantum chemical calculations.[10,11] Additionally, several recent experiments have analysed their photoelectron spectra[12] and their corresponding photodetachment probabilities once the anions are formed.[13,14]

The analysis of the corresponding mechanisms for this formation has been attempted less frequently since to put forward a realistic dynamical description of the path from neutral radicals, or from closed-shell chemical precursors, to the closed-shell stable anions has been more difficult. Hence, the recent studies have chiefly focused on the structural features of the final products, the latter task having already been an intriguing and complicated challenge.[10,11]

The aim of the present paper is therefore that of elucidating some features of the formation mechanism, or mechanisms, which we here relate to the unusually large values of permanent dipole moments which were found to exist along the C_nN^- series of stable negative ions.[3,10] In particular, we wish to analyse in some detail the bearing that such large, final dipole moments of the stable anionic valence bound states (VBSs) have on formation processes, chiefly among them being the direct route given by radiative electron attachment (REA):

$$C_nN + e^- \rightarrow C_nN^- + h\nu, \tag{1}$$

keeping in mind that most of the stable, ground-state VBS species have very large and positive electron affinities (EAs) and therefore the large exothermicity of the process (1) could also cause possible fragmentation via dissociative electron attachment (DEA) paths:

$$HC_nN + e^- \rightarrow C_nN^- + H \tag{2}$$

the above example is a fragmentation leading to the dehydrogenation process, while the larger fragmentation of an N-bearing carbon chain is given by Eq. (3):

$$NC_nN + e^- \rightarrow CN + C_{n-1}N^- \tag{3}$$

which would be responsible for the production of smaller terms in the series, whenever their EA values are larger than that of the CN fragment.

Regarding the generation of cyanoanions, one should also remember that more conventional chemical reactions have also been suggested:

$$C_n^- + N \rightarrow C_{n/2}N^- + C_{n/2}, \tag{4}$$

$$C_n^- + N \rightarrow CN^- + C_{n-1}, \tag{5}$$

which should dominate in the outer and middle parts of a C-rich envelope ($r \geq 10^{16}$ cm[15]), as well as the efficient fragmentation of the final VBS anions after DEA attachment processes:

$$C_nN + e^- \rightarrow C_{n-1}N^- + C \tag{6}$$

a possible chemical decay which turns out to be varying in efficiency along the series in an alternating manner with changes of n.[13]

Returning therefore to the primary process (1), a phase-space model put forward a while ago[16] suggested that the efficiency of the REA path to formation of VBS anions could be related to the phase-space distributions of the internal

a)Electronic mail: francesco.gianturco@uniroma1.it

rotovibrational modes of the final anion, while an even earlier modeling of the process was put forward by Clary and co-workers,[17,18] who suggested a capture approximation induced by the large dipole of the molecular targets. More recently, some of the present authors have carried out a more rigorous, multichannel treatment of the quantum scattering process implied by the lhs of Eq. (1) to obtain information on the formation of stable anions of linear polyynes of the C_nH^- type[19] by relating the attachment efficiency to the corresponding presence of metastable resonant states of the anions into the continuum of the low-energy spectrum. In the latter case, it was also suggested that the efficiency of the REA processes for highly polar targets can be enhanced by two important intermediate steps (i) dipole states in the near-threshold electron continuum, termed there dipole-scattering states (DSSs) and (ii) excited anionic states very near threshold which are known as dipole-bound states (DBSs).[20,21] The radiative stabilization occurring from the DSS to the DBS state, when existing, would involve a very large overlap between initial and final states, a very small energy dissipation gap and a large transition moment. All such elements contribute to the occurrence of large REA probabilities which would now be in efficient competition with autodetachment.[19,22]

In the present study we intend to further investigate the effects originating from dipole values above the known critical value of ∼1.67 D[22] on the electron attachment to the first few terms of the C_nN series ($n = 1$ to 7), examining both the permanent dipoles' sequence for the neutral radicals and that for the closed-shell VBS anions along the same series.

The work is organized as follows: Sec. II describes the results from structure calculations at the quantum chemical level of the several relevant properties of the two series: neutral radicals and stable closed-shell anions, while Sec. III describes our scattering quantum model to generate threshold electron wavefunctions in the meV range above the detachment thresholds. The results from both sets of calculations are reported and discussed in Sec. IV, while Sec. V present our conclusions.

II. STRUCTURAL CALCULATIONS

For the smallest member of the series, the CN radical, there is little experimental information on its permanent dipole, although several calculations exist on its value for the $CN(X^2\Sigma^+)$ ground state (for a recent overview of such calculations see Ref. 24). Their estimates range from 2.26 to 1.44 D, the last value obtained from extensive CASSCF-MRCI calculations,[23] which come close to the fairly old experimental value of 1.47 D.[24] The negative end of the dipole is located on the nitrogen atom, so that the direction of the dipole is negative along the z-axis which is taken to be pointing from the C to the N atom in the molecule. The radical's dipole therefore points towards the C-end of the molecule. Upon forming of the VBS anion, however, the permanent dipole moment strongly inverts its sign since the C-end becomes the negatively charged part of the molecule and the dipole value μ changes to positive at ∼0.7 D for the $CN^-(X^1\Sigma^+)$ ground state (see Table I for details of the calculation).

TABLE I. A summary of computed and experimental dipole moments (in Debye) and of Electron Affinities (EAs, in eV) for the present series of cyanopolyynes. Those marked by [*] are the results of the present calculations. See main text for further details.

Species	μ(expt.)	μ(calc.)	EA(expt.)	EA (calc.)
CN	−1.45[24]	−1.38[*] −1.44[27] −1.47[28]	+3.86[25]	+3.8[26] +3.82[28]
C_3N		−3.65[29] −3.00[*] −2.89[28] −2.79[31]	+4.59[30] +4.31[12]	+3.6[11] +4.40[29] +3.82[28]
C_5N		+0.80[*]		+4.59[10]
C_7N		+1.29[*]		+4.61[10]
CN^-		+0.69[*]		
C_3N^-		+3.10[11] +2.72[*]		
C_5N^-		+5.23[10] +4.19[*]		
C_7N^-		+7.54[10] +5.61[*]		

The vertical EA value comes from calculations and was found to vary between 2.59 and 3.83 eV,[27] close to the most recent experimental estimate of 3.860 ± 0.003 eV.[25] More recent calculations of the zero-point EA value[26] produced 3.8 eV. Thus, we see that, on forming the stable VBS anion this molecule undergoes a marked "swing" of its permanent dipole but does not possess a dipole value of the neutral which can support bound, excited DBS anions. Hence, the REA stabilization channel will not be able to take advantage of the physical intermediate steps we discussed in Sec. I.

As a matter of fact, the smallness of the relevant transition moment and the limited number of vibrational states in this element of the polyynes series have already been used to argue against the likelyhood of the REA path to CN^- formation,[26] while an alternative chemically reactive route:

$$H^- + HCN \rightarrow H_2 + CN^- \tag{7}$$

has been found in recent calculations using transition-state theory[32] to be around two orders of magnitude more efficient at temperatures around 10–100 K.

If we now turn to the next term of the series, the $C_3N(X^2\Sigma^+)$ radical, the relevant calculations for its permanent dipole moment vary between 2.32 and 3.25 D[29] depending on the quality of the chosen basis set expansion: the cc-pVTZ expansion with CAS-CI correlation corrections yielded 3.655 D, i.e., well beyond the critical dipole for the formation of DBS anions.[11] The dipole orientation is again along the negative z-axis of the molecule with the negative charge located on the nitrogen atom. Furthermore, the C_3N^- VBS has an EA value from calculations to be between 3.6 and 4.4 eV[11,29] and the most reliable experimental value[30] is about 4.59 eV. No experimental dipole moment is known for either the neutral or the anionic molecules, while calculations for the $C_3N^-(X^1\Sigma^+)$ electronic state[11] report a positive dipole

of 3.18 D, with the negative charge located at the C-end of the chain. Thus, on forming the VBS anion, also the C_3N radical undergoes a very marked change of its permanent dipole, so that a supercritical value is attained for both terms of the process within the REA path:

$$C_3N(X^2\Sigma^+) + e^- \rightarrow C_3N^-(X^1\Sigma^+) + h\nu. \qquad (8)$$

The next longer term of the series is given by the C_5N radical species. Its experimental dipole moment is also not known, but our *ab initio* calculations indicate the occurrence of an interesting reduction of the level of polarity between its two ends: the "through-bond" polarization of the N-atom lone pairs reduces the positive charge on the terminal carbon atom while also reducing the negative charge on the N-atom. The final dipole is now much smaller (+0.80 D), and its sign is inverted with respect to the one in the previous term of this series. It points now towards the positive terminal N atom. On formation of the VBS anion of the $C_5N^-(X^1\Sigma^+)$ ground electronic state, however, the dipole moment becomes strongly supercritical[10,12] while remaining positive; additionally, the zero-point EA value is again fairly large at 4.59 eV,[3,10] in keeping with the previous terms of the series. The much larger positive μ value is now 5.23 D,[10] and it is markedly supercritical.

The "through-bond" charge polarization effects are also confirmed by the calculations on the next term of the series, the $C_7N(X^2\Pi^+)$ radical. The permanent dipole moment of the system remains in fact fairly small (+1.29 D) and its sign also remains positive. The formation of $C_7N^-(X^1\Sigma^+)$ VBS anions once more produces a marked strengthening of the permanent dipole, which is now strongly supercritical: 7.54 D[3,10] while remaining positive, i.e., with negative charges on the carbon-end of the chain. The zero-point EA value is also very large: 4.61 eV,[3,10] in keeping with all previous terms in the series and with the large increase of the dipole value when going from the neutral radical to the VBS, closed-shell anion. The results discussed above are summarised by the data given in Table I.

The above structural information is already indicating an interesting evolution of the possible role that the permanent dipole values of the neutral radicals could have along the path to the anion formation by REA mechanism. From the $n = 1$ to the $n = 7$ terms of the series, in fact, only the neutral radical C_3N was shown to possess a supercritical dipole and therefore the possible role of intermediate, near-threshold anionic states both in the continuum (the DSS configurations mentioned earlier) and as weakly bound states, the DBS configurations below threshold.

To further find, albeit qualitatively, structural reasons for the variations of the dipole moment's size and value along the series of the neutral radicals, we have analysed specific features of the MO densities associated with the highest occupied molecular orbitals (HOMOs) of the radicals. The pictures reported in the two panels of Figure 1 show such orbitals for the first two terms of the series: the CN radical (upper panel) and the C_3N radical (lower panel).

The following comments can help us to confirm what suggested by our chemical intuition:

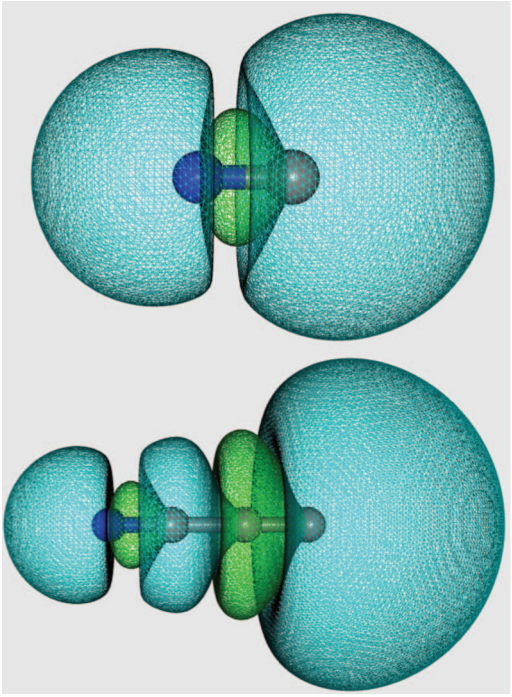

FIG. 1. Computed DFT electron densities of the HOMO orbitals in the neutral radical species, both in their $X^2\Sigma^+$ electronic states, of the CN molecule (upper panel) and the C_3N molecule (lower panel). See main text for further details.

(i) both orbitals clearly show marked σ-type nature, i.e., their densities are largely distributed along the skeleton of the intra-atomic bonds, with nodal planes perpendicular to the main axis. The density of this singly occupied MO also places the single radical's electron on the terminal C atom, as expected;

(ii) the presence of all the other, doubly occupied orbitals on the N-end of the molecule (describing the nitrogen lone-pair structure) causes the total charge to be largely located on the more electronegative N-atom, thus making its dipole, as discussed before, to point towards the C-end of the molecule;

(iii) the general "stiffness" of the σ-orbitals therefore largely prevents any through-bond polarisation of the radical electron towards the N-end of the molecule, thereby keeping charges apart. Both molecules, therefore, exhibit fairly large dipole moments controlled by standard electronegativity differences.

The features of the computed HOMO electron densities for the next two terms of the series are shown by the panels of Figure 2, where the corresponding density for the C_5N neutral is given by the upper panel and that for the C_7N is reported in the lower panel.

As opposed to what was shown by the data in Figure 1, our DFT calculations for both systems now indicate the total electronic configurations of both radicals to be given by $^2\Pi$ electronic states.

Earlier calculations[10] for the lowest electronic states of the four cyanopolyynes reported in our work had used the expansion of Dunning's correlation-consistent polarized valence quadruple-zeta basis set (cc-pVQZ set) plus the diffuse *s*, *p*, *d*, *f*, and *g* functions from the corresponding augmented basis set (i.e., the aug-cc-pVQZ expansion) which are

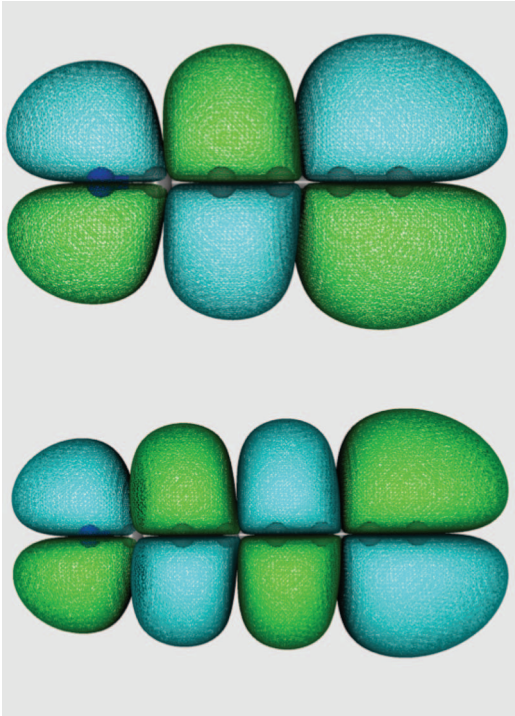

FIG. 2. Computed electron densities of the DFT HOMO orbitals in the neutral radical C_5N (upper panel) and in the neutral C_7N (lower panel). Both systems are in their $X^2\Pi$ ground electronic states. See main text for further details.

similar to the ones we have used in the present work (see data in Table I). They have employed them within a coupled-cluster single-double(triple) (CCSD(T)) post Hartree-Fock treatment of the correlation corrections. We have instead employed, in the calculations reported here, the Density Functional Theory (DFT) approach to correlation corrections. The *ab initio* treatment of Ref. 11 indeed confirmed that the electronic ground states of the CN and C_3N species are $X^2\Sigma^+$ states, while the C_5N is found there[11] to be still a cross-over species with nearly degenerate $^2\Sigma/^2\Pi$ ground states (the latter being lower in energy by ~0.02 eV). The calculations in Ref. 11 also find, like in our present work, a clearly $^2\Pi$ state for the C_7N radical and for the larger radical cyanopolyynes up to $C_{11}N$.[11]

Thus, we can say that our present calculations confirm the trend shown in earlier calculations,[11] and place the C_5N species already as a stable $^2\Pi$ state for its ground electronic configuration. This is a reassuring result, although we are also aware of the fact that the DFT calculations usually tend to overstabilize radical and anionic species,[21] and are also known to underestimate the computed permanent dipoles,[11] as shown in Table I.

The orbitals on the panels of Figure 2 therefore exhibit a very clear π-like character, with nodal planes along the main axis. Thus, contrary to the previous instances of Figure 1, the lobes of the densities over the chain of the carbon atoms could be more easily polarized towards the electronegative N-atom via the so-called "through-bond" polarization effect. The result of such "charge-transfer" feature could therefore be the reason for the changes in size and orientation of the permanent dipoles of the neutral radicals, as found in our calculations of Table I for the present molecules. This is in contrast with what occurs in the CN and C_3N species, where the dominant σ-character of the singly occupied orbitals prevents such polarization effects, thereby hindering charge migration within those molecules.

In conclusion, all existing calculations on the VBS of the ground-state, stable anions,[10,11,27,29] including the present ones, find that their ground electronic states are $^1\Sigma^+$ closed-shell configurations. It was also found earlier, and we have discussed these aspects in Sec. II, summarising the current findings in Table I, that upon the attachment of the extra-electron to the neutral radicals, the corresponding permanent dipole moment "swings" to the positive direction and increases markedly in size. This indicates that the negative charges are now localized on the carbon-end of these cyanopolyynes and that the size of such charges greatly increases from their neutral radical counterparts. We have also found in the previous analysis that only the CN and the C_3N neutral molecules have $^2\Sigma$ ground states, while C_5N, C_7N, and all the longer C_nN radicals[11] exhibit $^2\Pi$ configurations for their ground electronic states, with the C_5N molecule being the cross-over species with a small energy degeneracy between $^2\Sigma$ and $^2\Pi$ configurations.[11,12]

In order to further investigate, albeit on a qualitative level, the features of the lowest virtual orbitals of the radicals as possible indicators of what should happen with the charges in their corresponding anions, we report in Figures 3 and 4 the spatial electronic densities of the lowest unoccupied molecular orbitals (LUMOs) in CN and C_3N (Figure 3) and in C_5N and C_7N (Figure 4).

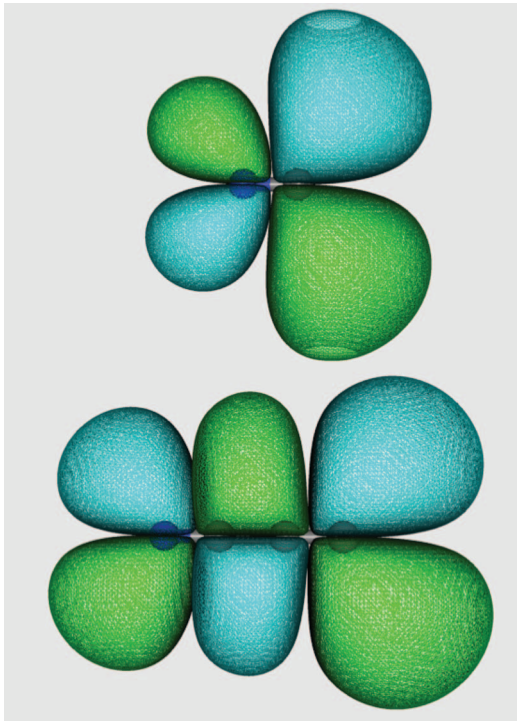

FIG. 3. Computed electron densities of the lowest virtual orbitals (LUMOs) for the neutral radicals CN($X^2\Sigma^+$) and C_3N($X^2\Sigma^+$) from the DFT calculations described in the main text. Upper panel: CN; lower panel: C_3N.

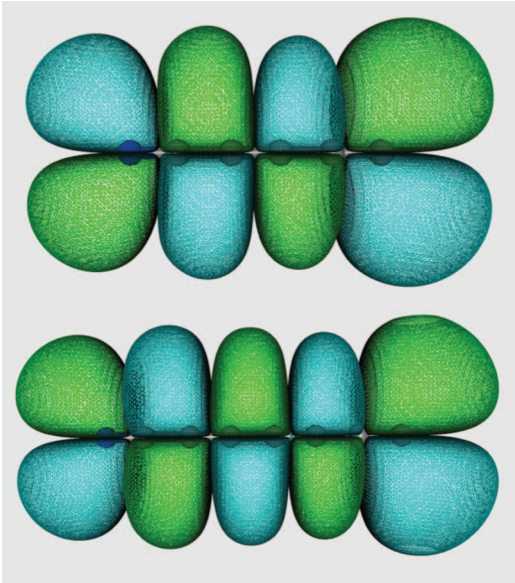

FIG. 4. Same computed electron densities as those in Figure 3, but for the C_5N and C_7N $^2\Pi$ electronic states of the neutrals. See main text for further details.

The following comments can be made from a perusal of the results reported in the figures:

(i) all virtual MOs which can play a role in polarization effects, triggered by the configuration-mixing which takes place during the electronic rearrangements occurring once the extra-electron is attached to the initial SOMO, have clear π*-like character along the whole series of cyanopolyynes, in contrast with σ-like character exhibited by the singly-occupied MOs (SOMOs) shown for the CN and C_3N radicals and discussed before;

(ii) since the additional electron, when forming the ground-state anionic species, will double the occupation of the SOMO which is largely localized on the C-end of the molecule, the final charges will be now strongly located in that region of the molecules, while the π*-like characters of the LUMOs reported here will favour further polarization of charges into that part of the stable anions;

(iii) the net effect will therefore be, as already found in the previous discussion, that the negative end of the charges will move towards the end-carbon atom and the values of the separated charges will further increase: all stable VBS anions therefore exhibit large dipole values pointing to the nitrogen-end of the cyanopolyynes;

(iv) a further role of such virtual orbitals will also be that of describing possible excited anionic states of the molecules, where both σ and π configurations, in either singlet or triplet states, have already been observed in earlier calculations.[27,29] In the present work, however, we shall investigate the special features of such states only for the case where a supercritical dipole moment exists in the neutral radical, i.e., for the C_3N.

The formation of the anions via electron attachment processes at low relative energies, as it is expected to occur in the ISM environments with the free electrons available in molecular clouds and in carbon rich stars,[5–8] will therefore be now analysed via actual quantum scattering calculations of the threshold electrons from their distribution in the ISM continuum environment.

Section III will therefore outline our computational approach to mapping the near-threshold scattered electrons by generating them from realistic calculations involving the present polyatomic targets.

III. THE SCATTERING CALCULATIONS: AN OUTLINE OF THE PRESENT MODEL

Since the quantum dynamical equations used for this study have been described in detail many times before,[33] we only present here a brief outline of it and refer the reader interested in more details to those publications.[19] The total (N+1)-electron wavefunction is constructed as an anti-symmetrized product of one-electron wavefunctions obtained from Hartree-Fock orbitals of the neutral ground state molecular target, considering the N bound electrons in their ground-state configuration during the whole scattering process: thus, no core-excited resonances are allowed in our modeling. Each of the three dimensional wavefunctions describing a given electron is expanded around the molecular center of mass (Single Center Expansion, SCE) so that for each of the bound molecular electrons we have

$$\phi^{p\mu}(r,\hat{\mathbf{r}}|\mathbf{R}) = \sum_{\ell h} \frac{1}{r} u^{p\mu}_{\ell h,i}(r|\mathbf{R}) \chi^{p\mu}_{\ell h}(\hat{\mathbf{r}}) \tag{9}$$

and for the scattered particle

$$\psi^{p\mu}(r,\hat{\mathbf{r}}|\mathbf{R}) = \sum_{\ell h} \frac{1}{r} f^{p\mu}_{\ell h}(r|\mathbf{R}) \chi^{p\mu}_{\ell h}(\hat{\mathbf{r}}). \tag{10}$$

In the above SCE representations, the superscripts label the μth irreducible representation of the pth symmetry group to which the molecule belongs at the fixed nuclear geometry $\mathbf{R}$, and the subscripts refer to each of the angular channels under consideration; the radial coefficients $u^{p\mu}_{\ell h,i}$ for the bound molecular electrons are numerically evaluated by a quadrature on a radial grid. The angular functions $X^{p\mu}$ are given as

$$\chi^{p\mu}_{\ell h}(\hat{\mathbf{r}}) = \sum_{m} b^{p\mu}_{\ell h m} Y_{\ell m}(\hat{\mathbf{r}}), \tag{11}$$

where the coefficients $b^{p\mu}_{\ell m h}$ were described and tabulated earlier.[34] The ensuing coupled partial integro-differential quantum scattering equations evaluate the unknown radial coefficients $f^{p\mu}_{\ell h}$ for the (N+1)th continuum electron:

$$\left[\frac{d^2}{dr^2} - \frac{\ell(\ell+1)}{r^2} + 2(E-\epsilon)\right] f^{p\mu\alpha}_{\ell h}(r|\mathbf{R}) = 2\sum_{\ell' h'} \int dr' V^{p\mu}_{\ell h,\ell' h'}(r,r'|\mathbf{R}) f^{p\mu}_{\ell' h'}(r'|\mathbf{R}), \tag{12}$$

where E is the collision energy and ϵ is the electronic eigenvalue for the found state energy so that $k^2/2 = E$, k being the asymptotic momentum of the elastically scattered electron. For a target which has an open shell electronic structure, with n_{occ} = (N−1)/2 *doubly* occupied molecular orbitals, the static-exchange (SE) potential has the following

form:

$$V_{SE} = \sum_{\gamma=1}^{M} \frac{Z_\gamma}{|\mathbf{r} - \mathbf{R}_\gamma|} + \sum_{i=1}^{n_{occ}} (2\hat{J}_i - \hat{K}_i)$$

$$= V_{st} - \sum_{i=1}^{n_{occ}} \hat{K}_i, \quad (13)$$

where $\hat{J}_i$ and $\hat{K}_i$ are the usual static potential and the non-local exchange potential operator, respectively. The singly occupied orbital of the radical is treated instead with its single occupancy, further considering the exchange as an average effect between singlet and triplet interaction with the (N+1) scattering electron.[19,35] We further model the correlation and polarization effects via the following optical potential:

$$V_{cp} = V_{corr}(r), r \leq r_{match}, \quad (14)$$

$$V_{cp} = V_{pol}(r), r > r_{match}, \quad (15)$$

employing density related models which have been described before for the short-range correlation effects.[33] We then generate the exchange interaction with the Free-Electron-Gas-Exchange model proposed by Hara (HFEGE[36]), V_{HFEGE}:

$$V_{HFEGE} = -\frac{2K_F(\mathbf{r}|\mathbf{R})}{\pi}\left[\frac{1}{2} + \frac{1-\eta^2}{4\eta}\ln\left(\frac{1+\eta}{1-\eta}\right)\right]. \quad (16)$$

When dealing with open-shell systems as the present case, the electronic density $\rho(\mathbf{r}|\mathbf{R})$ is modified to treat the radical electron as singly-occupied.[35] This final potential provides the so-called static-model-exchange-correlation-polarization (SMECP) potential accounting for the interaction forces between the inpinging free electron and the target molecule. The coupled set of integro-differential equations now takes the form:

$$\left[\frac{d^2}{dr^2} - \frac{\ell_i(\ell_i+1)}{r^2} + k^2\right] f_{\ell h}^{p\mu}(r)$$

$$= 2\sum_{\ell' h'} V_{\ell h,\ell' h'}^{p\mu}(r) f_{\ell' h'}^{p\mu}(r), \quad (17)$$

where the potential coupling elements are

$$V_{\ell h,\ell' h'}^{p\mu} = \left\langle \chi_{\ell h}^{p\mu}(\hat{r}) \middle| V(\mathbf{r}) \chi_{\ell' h'}^{p\mu}(\hat{r}) \right\rangle$$

$$= \int d\hat{r}\, \chi_i^{p\mu}(\hat{r}) V(\mathbf{r}) \chi_j^{p\mu}(\hat{r}). \quad (18)$$

The numerical solutions of the coupled equations produce the relevant K-matrix elements which will in turn yield the final integral cross sections.[33]

We have further tested a different, short-range correlation potential that has turned out to be very effective for highly correlate π-systems as those in the present series. We have therefore employed the V_{cp} form suggested by Padial and Norcross (PN[37]) and further employed by us in earlier studies.

The results of the present calculations, and the details of the actual numerical treatment, will be reported and discussed in Sec. IV.

IV. RESULTS AND DISCUSSION

A. The threshold scattering of electrons

As mentioned in the Introduction and in Secs. II and III, we have established from structural calculations that in the present series of cyanopolyynes, the permanent dipole moments of the initial neutral radicals indicate that only the C_3N molecule has a supercritical value of it, while the CN element of the above series is close to 1.67 D but below that threshold. The other longer members, e.g., C_5N and C_7N, have much smaller dipoles. On the other hand, all the members of the present series are seen to have much larger, supercritical dipoles when the corresponding closed-shell VBS anions are formed. In the case of CN and C_3N there is also a marked inversion on the orientations of the final dipoles. One should always remember, however, that this process describes only the ground-states of the stable molecular anions, while the dipole-driven anions will correspond to excited anionic states, as we shall further discuss below.

In an earlier, similar study on the formation of negative ions of polyynes,[19] we had analysed for several radical systems, which had supercritical dipoles in their electronic ground states (linear geometries), the behaviour of the scattering states of threshold electron with respect to the spatial geometry of the target atoms at the molecular equilibrium configurations.

We are therefore analysing now the same energy range above threshold for CN, C_3N, C_5N, and C_7N in order to explore the effects of the long range dipole potentials on the positioning of the scattered electron with respect to the molecular equilibrium structures of the neutral radicals.

The target wavefunctions for the system were given by DFT calculations by using the aug-cc-pVTZ basis set and the corresponding equilibrium geometries were also optimized during the calculations at the same level: their values are given in Table II.

The scattering calculations involved a multipolar expansion of the potentials up to L_{max}= 140, while the scattered electron's partial-wave expansion extended up to l_{max} = 70. The outer integration's radial matching was done at R_{out} = 500, while the inner region, where all potentials terms of short-range nature were included, extended up to R_{in} = 50.

The two panels of Figure 5 report the more nearby regions of spatial shapes of the scattering electron's wavefunctions for the first two terms of the series: CN($X^2\Sigma^+$) and C_3N($X^2\Sigma^+$).

The calculated wavefunctions correspond to scattering energies of 1 meV above threshold, although in both cases a similar behaviour of the scattering wavefunctions can be

TABLE II. Optimized equilibrium geometries of the target neutral radicals.

Radical	R_{N-C_1}	$R_{C_1-C_2}$	$R_{C_2-C_3}$	$R_{C_3-C_4}$	$R_{C_4-C_5}$	$R_{C_5-C_6}$	$R_{C_6-C_7}$
CN	1.162						
C_3N	1.155	1.368	1.204				
C_5N	1.162	1.347	1.233	1.314	1.286		
C_7N	1.161	1.350	1.227	1.318	1.246	1.305	1.285

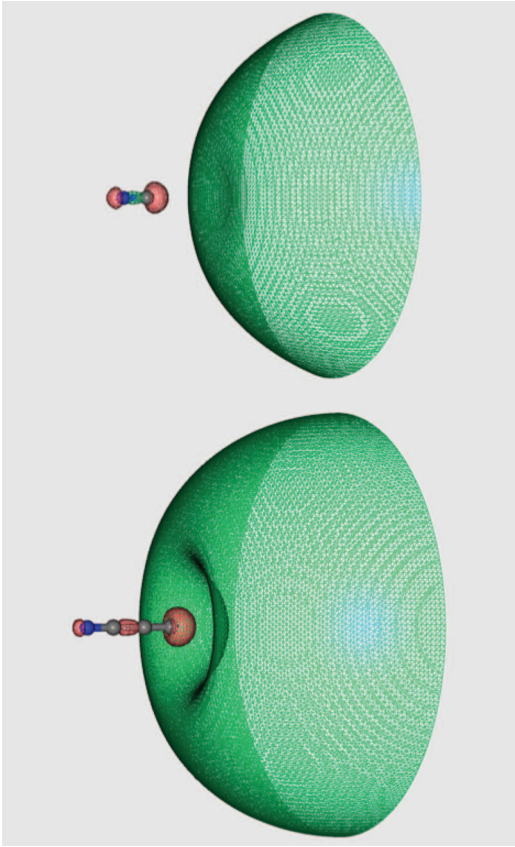

FIG. 5. Computed real parts of the scattering electron's wavefunctions mapped over the 3D space of the atomic configurations of the target molecules. Top panel: CN($X^2\Sigma^+$) as a target; lower panel: $C_3N(X^2\Sigma^+)$ as a target. See main text for further details. The molecular axis has the N atom end on the left for each molecular target. Only a partial view of the spherical regions is presented in both panels.

observed as higher up as 100 meV or so. The following observations could be made:

(i) although the CN target was found to have a subcritical dipole strength, we have no experimental confirmation of its value while different computational treatments provide final dipole values also above that threshold. This indicates that the polar CN target could show nearly-critical dipole scattering behaviour;

(ii) as a result of this dipole value, we notice in the top panel of Figure 5 that the scattering wavefunction is really dominated by the $\ell = 1$ partial-wave component as a very large region of it is placed outside the molecule at its positive end (the carbon side) while a nodal surface indicates a more compact region around, and close to, the C atom in the target. Hence, in spite of the presence of many more partial-waves being coupled to each other within the calculations, the scattering of this near-threshold electron is dominated by the dipole potential and it is located largely outside the molecular space: such features are the pictorical indicators of a dipole-scattering state (DSS) configuration, as outlined before and as already discussed earlier by us for other systems;[19]

(iii) the lower panel of Figure 5 reports similar calculations for the $C_3N(X^2\Sigma^+)$ target in its ground electronic state. The scattering energy is the same as before and we clearly see the very similar behaviour of the relevant scattered electron: large localization outside the molecular framework on the positive side of the dipole (the C-end of the molecule), a nodal surface (from the $\ell = 1$ dominant component of the dipole driven scattering) close to the end-carbon side, and very little residual density of the extra electron all along the molecular chain of bonds. Both scattering states now describe sigma states of the anionic complex in the continuum.

The above findings thus suggest that, given the nature of the polarity in both targets, the possibility exists that any environmental electron in the ISM could interact with both species in the special form reported above. This means, therefore, that metastable anionic states could be formed in the continuum from impinging electrons which have relative energies at the colder end of their distribution (e.g., a few kelvin of temperature). As a consequence of their special features, therefore, one may consider such DSS configurations as now providing new special doorways to possible anion stabilization paths, as we shall further discuss below.

Our further calculations on the next two molecules of the cyanopolyynes discussed in the present work are shown in Figures 6 and 7.

The following comments could be made from results reported in the first of the above figures in relation to the possible existence of DSS configurations for threshold-energy electron scattering off C_5N target molecules:

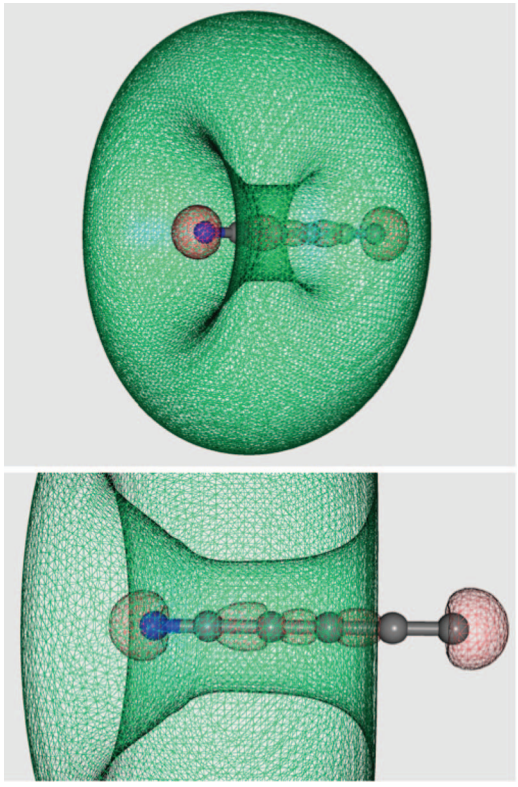

FIG. 6. Computed real part of the threshold scattering electron's wavefunction at a collision energy of 1 meV and for the $C_5N(X^2\Sigma^+)$ target molecule. The top panel shows the molecular frame along the z-axis with the N-atom and coming out of the figure plane. Lower panel: same as in the upper panel, but with the main axis on the figure plane and the C-end atom on the right. The threshold scattering wavefunction is now additionally enlarged to allow the reader to note the phase's changes along the linear carbon chain. See main text for further details.

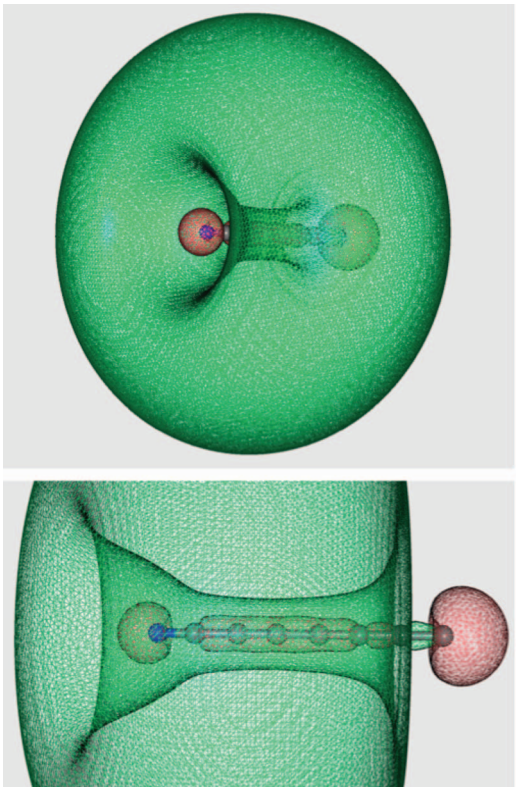

FIG. 7. Computed real part of the scattered electron's wavefunction at a collision energy of 1 meV and for the C_7N target neutral radical. The two panels are the same as in Figure 6, so that in the upper one the molecular frame is along the z-axis with the N-atom and coming out of the figure plane. Lower panel: same as in the lower panel of Figure 6. See main text for further details.

(i) the permanent dipole of the neutral radical has now changed sign with respect to the previous two terms of the series: its positive end is on the N atom while the C-end of the molecule is the negative one. Furthermore, our calculations indicate that the size of this dipole has now reduced to about 1/4 of the value of the C_3N permanent dipole, thereby becoming much smaller than the threshold value of 1.67 D;[22]

(ii) the corresponding wavefunction is therefore not produced by dominant, dipole-driven scattering potential but it is due to also additional contributions from higher-order, short-range multipoles which therefore play a greater role in this system. As a consequence, we do not see it localized outside the molecule and on the positive end of the dipole: we clearly see, instead, that the nodal surface becomes more complicated and seems to have $\ell = 2$ contributions around the main molecular axis and along the molecular bonds;

(iii) the interplay of the different angular dependencies of at least three partial-waves that become now important ($\ell = 0$, 1, and 2) are shown even more clearly by the view of the present threshold wavefunction reported by the lower panel of Figure 6. We see there that the threshold-energy wavefunction has at least two nodal surfaces and that it is brought in closer to the molecular structure, over the sequence of molecular bonds which start at the nitrogen side and along the C–C bonds. One can therefore say that such configurations are very close to the molecular structure and do not resemble at all the external DSS states seen for the previous molecular targets.

That a similar behaviour is also carried over to the next larger molecule of the cyanopolyyne series could be seen from the additional calculations for the threshold scattering wavefunction of the metastable anion for the C_7N as given in Figure 7.

As discussed before, we have seen that the permanent dipole moment of this neutral radical remains positive and therefore indicates the carbon end as negatively charged. Furthermore, the "through-bond" polarization that we had mentioned before is also occurring in this molecule, so that its dipole is now smaller and points to the N-end of this cyanopolyyne. The corresponding near-threshold scattering wavefunction (real part) of Figure 7 resembles that observed in Figure 5: in fact, it seems to accumulate on the nitrogen side (the positive side) of the molecule, as additionally expected. Thus, the higher terms of the multipolar potential are also playing an important role here and contribute as much as the dipole-charge interaction. As a result of it, we see that the scattering electron's wavefunction now accumulates along the bonds inside the carbon chain and exhibits additional nodal surfaces due to the role of the $\ell = 2$ contributions to the partial-wave description of the threshold electron.

In conclusion, we see from the above calculations that only the C_3N^- and the CN^- systems can give rise to metastable anionic states above threshold that have all the features of dipole-driven scattering states. Such intermediate configurations could therefore play a significant role in REA processes into the next intermediate anion below threshold: the DBS states. However, we have discussed earlier that the CN molecule has a dipole moment below the critical value and therefore the existence of a DBS configuration for a bound anion have not in fact been found.

B. The search for dipole-bound states of C_3N^-

Earlier calculations on the CN^- and C_3N^- systems about the possible existence of bound, excited anions which could be described as DBS configurations[28] indicated that the neutral radicals possess a supercritical (C_3N) and nearly critical (CN) dipole moment but also suggested that neither molecule exhibits an excited anionic state which could be described as a dipole-driven bound state. On the other hand, similar calculations by Harrison *et al.*[27,29] confirmed the lack of such states for CN^-, but found, however, that the C_3N^- has indeed a series of four $^3\Sigma^+$ excited anions, the least bound of which exhibits a binding energy of 1.2 meV, well above the other three triplet states of Σ character which they also listed between their highest excited state and the VBS anion at around 4 eV of binding energy (see Table VI in Ref. 30). They also found a $^1\Pi$, $^3\Pi$ state with a binding energy of 0.3 meV (see Table VI in Ref. 30). No mention of their possible DBS nature was made in that work. The LUMO maps given by our DFT calculations reported by Figures 3 and 4 could qualitatively represent some of these possible excited anionic states, like those discussed in Ref. 29.

The results from our present calculations for the DBS wavefunction of the $C_3N^-(^3\Sigma)$ electronic configuration are reported by Figure 8. They show the spatial form of the extra

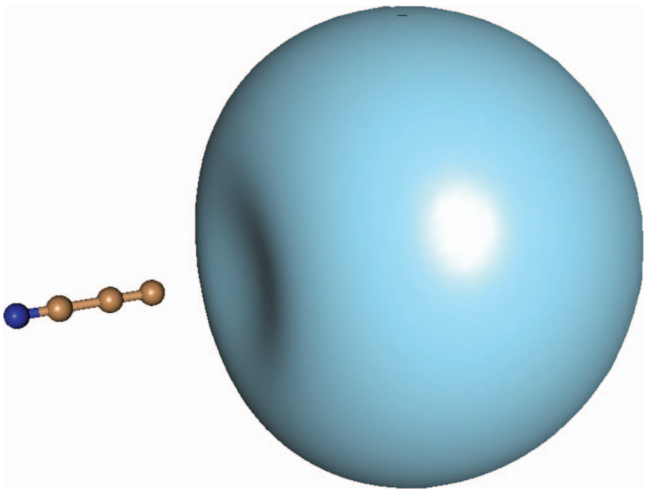

FIG. 8. Spatial distribution of the bound, singly-occupied MO for the excited anion produced by the calculations of a DBS state. See main text for further details.

electron now weakly bound to the C_3N molecule. The weakly bound electron's wavefunction is clearly shown to be essentially the same as in the DSS state involving the scattering electron off the neutral radical, as given by the lower panel of Fig. 5. We further find that the nuclear geometry is essentially the same in both molecules since such attached electron hardly modifies the spatial stabilization of the molecular atoms. The energy value was obtained from ROHF calculations which made use of a large basis set (aug-cc-pVTZ) to which we added an additional string of diffuse functions given by an even-tempered basis set with exponents produced via the formula $2 \times 10^5 \times (3.2)^n$, with $n = 2, 7$, as already discussed and employed in our earlier work.[19] These calculations, besides providing the spatial indicator of a DBS state as shown in Fig. 8, yielded a binding energy for that diffuse electron of 0.33 meV not far from the earlier estimates of 1.2 meV for the binding energy of the extra electron in the excited anion[29] as already discussed above. In that work, however, the MRCI-CC calculations did not allow to produce similar spatial maps of the relevant MO's, so that no reference was made to their possible nature as weakly bound DBS anionic state of the C_3N^- system. One should note again the strong similarity between the bound wavefunction of the DBS electron of Figure 8 and the DSS state of a threshold electron reported for the same molecule in the lower panel of Figure 5. This specific feature of these two extra electrons above and below the energy threshold will be further discussed in Sec. V.

V. PRESENT CONCLUSIONS

In the present work we have analysed the links existing between specific structural properties of a series of N-bearing carbon chains (the cyanopolyynes) and their possible paths to formation in the ISM and in the outer regions of carbon-rich stars as stable anionic molecules.

The work has been focused on the feasibility of the formation mechanism by direct radiative electron attachment reactions,

$$C_nN + e^- \rightarrow C_nN^- + h\nu, \qquad (19)$$

and we have looked at the role that the permanent dipole moments of the initial radical partners could have in stabilizing the ground-state VBS anions of the title molecules, in successful competition with auto-detachment channels.

The structural calculations reported in Sec. II have revealed that only the C_3N member of the series has a supercritical (>1.67 D) permanent dipole in its ($^2\Sigma^+$) neutral ground state. The smallest member, the CN partner, has a near-critical dipole depending on the quality of the computations employed (see Table I). Furthermore, all calculations on the corresponding closed shell anions C_nN^- indicated that the VBS anionic states have very large, supercritical dipole moments, with the negatively charged regions around the terminal carbon atoms.

Our results indicate that, upon electron attachment to the initial neutral radicals the systems undergo marked structural changes which are strongly linked with electronic rearrangement effects, occurring during the transition from neutral radicals to closed-shell, valence-type anionic structures.

The confirmed existence, for all the systems considered, of rather large and positive EA values further indicates that in cyanopolyynes a substantial amount of energy release is expected to take place on the formation of VBS structures. When such a feature is also tied up with the computational evidence of the existence of metastable resonant anionic states fairly high-up in the energy continuum (e.g., see Refs. 27 and 29) and not near threshold, then it becomes plausible to expect that direct REA paths would be likely to induce bond breaking effects into smaller species or to be causing very small transition probabilities as for CN^-.[26]

The additional quantum dynamical calculations that we have carried out for all the title systems in Sec. IV indicate a realistic alternative for the path to the anionic formation in the ISM: the presence of threshold scattering states in cases when the radical's permanent dipole is larger than the critical threshold of 1.67 D.[20,21] Such states are describing an outer electron within the metastable anion which is very similar in shape, angular structure and location, around the neutral partner, as an excited, anionic bound state **below** threshold which identifies the presence of a DBS state.

Thus, the present physical scenario allows us to conclude that those polar radicals which satisfy the supercritical conditions of their permanent dipoles possess a more efficient path to VBS formation: the formation of intermediate near-threshold anions (above and below the energy threshold) which the continuum electron can easily employ for highly efficient REA paths. Such intermediate states reach then by intramolecular vibrational relaxation (IVR) processes the final VBS anion with the less likely occurrence of molecular fragmentations. The latter step is the one invoked in the earlier phase-space models[16] and in our resonant intermediate models,[19] one that is here indicated to occur in competition with the autodetachment from an excited bound state of the anions (their DBS configurations). Of the molecules examined in the present work, we have shown that only the C_3N radical has the necessary features for following the present path to stabilization via intermediate anions, as graphically described in Figure 9.

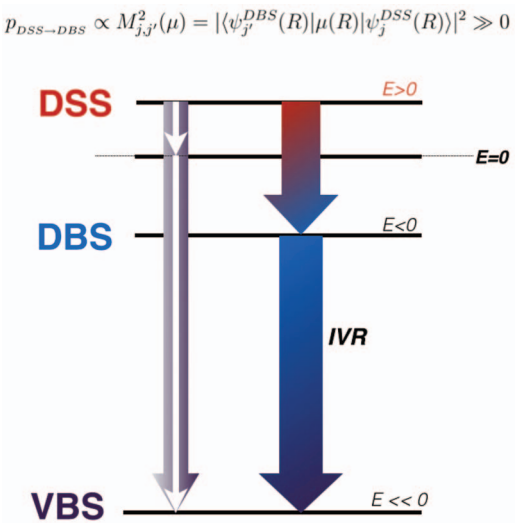

FIG. 9. Schematic view of the electron attachment process into a VBS anionic configuration for the case of the C_3N^- system. The expected form of the transition dipole moment is indicated on top of the scheme. See main text for further details.

In the same figure we also outline the qualitative form of the transition dipole moment (TDM) coupling operator associating the initial and final anions as the relevant intermediates to the VBS formation.

One should also add here that, although we have shown that the CN molecule could have DSS configurations above threshold, that system does not have intermediate DBS anions and therefore its corresponding TDM, as already shown in Ref. 26, is too small to efficiently compete with the autodetachment channels. Furthermore, our recent analysis[32] of reaction (7) has shown the latter to be a more efficient alternative to the direct REA process of Eq. (1).

In conclusion, therefore, our present study has shown the important role played on anionic stabilization process by the permanent dipole moments of the neutral, radical partners. Our calculations indicate that the formation of metastable, excited anions near the energy threshold of the incoming electrons (above and below that threshold) could provide efficient intermediate steps on the path to forming the stable anionic VBS configurations observed in the ISM for such molecules.

ACKNOWLEDGMENTS

We gratefully acknowledge support from the Austrian Science Foundation (FWF). We also want to thank S. Kumar for helpful discussions on neutral open shell systems.

[1]J. D. Watts and R. J. Bartley, J. Chem. Phys. **97**, 3445 (1992).
[2]D. Forney, J. Fulara, P. Freivogal, M. Jakobi, D. Lessen, and J. P. Maier, J. Chem. Phys. **103**, 48 (1995).
[3]Chang-Guo Zhan and S. Iwata, J. Chem. Phys. **104**, 9058 (1996).
[4]D. Zajfman, H. Feldman, D. Heber, O. Kella, D. Maier, Z. Vager, and R. Naaman, Science **258**, 1129 (1992).
[5]K. Kawaguchi, Y. Kasai, S. Ishikawa, and N. Kaifu, Publ. Astron. Soc. Jpn. **47**, 853 (1995).
[6]K. Kawaguchi, R. Fujimori, S. Aimi, S. Takano, E. Y. Okabayashi, H. Gupta, S. Brunken, C. A. Gottlieb, M. C. McCarthy, and P. Thaddeus, Publ. Astron. Soc. Jpn. **59**, L47 (2007).
[7]P. Thaddeus, C. A. Gottlieb, H. Gupta, S. Brunken, M. C. McCarthy, M. Agundez, M. Guelin, and J. Cernicharo, Astrophys. J. **677**, 1132 (2008).
[8]M. C. McCarthy, C. A. Gottlieb, H. Gupta, and P. Thaddeus, Astrophys. J. **652**, L141 (2006).
[9]T. Pino, M. Tulej, F. Guether, M. Pachkov, and J. P. Maier, J. Chem. Phys. **116**, 6126 (2002).
[10]P. Botschwina and R. Oswald, J. Chem. Phys. **129**, 044305 (2008).
[11]R. Kołos, M. Gronowski, and P. Botschwina, J. Chem. Phys. **128**, 154305 (2008).
[12]T. A. Yen, E. Garand, A. T. Sereve, and D. M. Neumark, J. Chem. Phys. **114**, 3215 (2010).
[13]T. Best, R. Otto, S. Trippel, P. Hlavenka, A. von Zastrow, S. Eisenbach, S. Jezovin, R. Wester, E. Vigren, M. Hamberg, and W. D. Geppert, Astrophys. J. **742**, 63 (2011).
[14]S. S. Kumar, D. Hauser, R. Jindea, T. Best, S. Roucka, W. D. Geppert, T. J. Millar, and R. Wester, Astrophys. J. **776**, 25 (2013).
[15]M. A. Cordiner and T. J. Millar, Astrophys. J. **697**, 68 (2009).
[16]N. Harada and E. Herbst, Astrophys. J. **685**, 272 (2008).
[17]D. C. Clary and J. P. Henshaw, Int. J. Mass Spectrom. **80**, 31 (1987).
[18]D. C. Clary, J. Phys. Chem. **92**, 3173 (1988).
[19]F. Carelli, M. Satta, T. Grassi, and F. A. Gianturco, Astrophys. J. **774**, 97 (2013).
[20]C. Desfrançois, Phys. Rev. A **51**, 3667 (1995).
[21]J. Simons, J. Phys. Chem. A **112**, 6401 (2008).
[22]W. R. Garrett, J. Chem. Phys. **77**, 3666 (1982).
[23]S. R. Polák and J. Fiser, J. Mol. Struct. **584**, 69 (2002).
[24]R. Thomson and F. W. Dalby, Can. J. Phys. **46**, 2815 (1968).
[25]S. E. Bradforth, E. H. Kim, D. W. Arnold, and D. M. Neumark, J. Chem. Phys. **98**, 800 (1993).
[26]N. Douguet, S. Fonseca dos Santos, M. Raoult, O. Dulieu, A. E. Orel, and V. Kokoouline, Phys. Rev. A **88**, 052710 (2013).
[27]S. Harrison and J. Tennyson, J. Phys. B.: At. Mol. Opt. Phys. **45**, 035204 (2012).
[28]R. C. Fortenberry and D. T. Crawford, J. Chem. Phys. **134**, 154304 (2011).
[29]S. Harrison and J. Tennyson, J. Phys. B.: At. Mol. Opt. Phys. **44**, 045206 (2011).
[30]K. Graupner, T. L. Merrigan, T. A. Field, T. G. A. Youngs, and P. C. Marr, New J. Phys. **8**, 117 (2006).
[31]P. Botschwina, M. Haru, J. Fluegge, and S. Seeger, J. Chem. Soc., Faraday Trans. **89**, 2219 (1993).
[32]M. Satta, F. A. Gianturco, F. Carelli, and R. Wester, "Exploring a chemical path for CN- formation in the Interstellar Medium," (to be submitted).
[33]R. R. Lucchese and F. A. Gianturco, Int. Rev. Phys. Chem. **15**, 429 (1996).
[34]S. L. Altmann and H. P. Cracknell, Rev. Mod. Phys. **37**, 19 (1965).
[35]F. Carelli and F. A. Gianturco, Eur. Phys. J. D **67**, 268 (2013).
[36]S. Hara, J. Phys. Soc. Jpn. **22**, 710 (1967).
[37]N. T. Padial and D. W. Norcross, Phys. Rev. A **29**, 1742 (1984).